Title
Clinical implementation of intrafraction cone beam computed tomography imaging during lung tumor stereotactic ablative radiation therapy.

Journal
International Journal of Radiation: Oncology - Biology - Physics, 87(5)

Authors
Li, Ruijiang
Han, Bin
Meng, Bowen
et al.

Publication Date
2013-12-01

DOI
10.1016/j.ijrobp.2013.08.015

Peer reviewed

Published in final edited form as:
Int J Radiat Oncol Biol Phys. 2013 December 1; 87(5): 917–923. doi:10.1016/j.ijrobp.2013.08.015.

Clinical Implementation of Intrafraction Cone Beam Computed Tomography Imaging During Lung Tumor Stereotactic Ablative Radiation Therapy

Ruijiang Li, PhD[*], **Bin Han, PhD**[*], **Bowen Meng, MS**[*], **Peter G. Maxim, PhD**[*,†], **Lei Xing, PhD**[*,†], **Albert C. Koong, MD, PhD**[*,†], **Maximilian Diehn, MD, PhD**[*,†,‡], and **Billy W. Loo Jr, MD, PhD**[*,†]

[*]Department of Radiation Oncology, Stanford University School of Medicine, Stanford, California

[†]Stanford Cancer Institute, Stanford University School of Medicine, Stanford, California

[‡]Institute for Stem Cell Biology and Regenerative Medicine, Stanford University School of Medicine, Stanford, California

Abstract

Purpose—To develop and clinically evaluate a volumetric imaging technique for assessing intrafraction geometric and dosimetric accuracy of stereotactic ablative radiation therapy (SABR).

Methods and Materials—Twenty patients received SABR for lung tumors using volumetric modulated arc therapy (VMAT). At the beginning of each fraction, pretreatment cone beam computed tomography (CBCT) was used to align the soft-tissue tumor position with that in the planning CT. Concurrent with dose delivery, we acquired fluoroscopic radiograph projections during VMAT using the Varian on-board imaging system. Those kilovolt projections acquired during megavolt beam-on were automatically extracted, and intrafraction CBCT images were reconstructed using the filtered backprojection technique. We determined the time-averaged target shift during VMAT by calculating the center of mass of the tumor target in the intrafraction CBCT relative to the planning CT. To estimate the dosimetric impact of the target shift during treatment, we recalculated the dose to the GTV after shifting the entire patient anatomy according to the time-averaged target shift determined earlier.

Results—The mean target shift from intrafraction CBCT to planning CT was 1.6, 1.0, and 1.5 mm; the 95th percentile shift was 5.2, 3.1, 3.6 mm; and the maximum shift was 5.7, 3.6, and 4.9 mm along the anterior-posterior, left-right, and superior-inferior directions. Thus, the time-averaged intrafraction gross tumor volume (GTV) position was always within the planning target volume. We observed some degree of target blurring in the intrafraction CBCT, indicating imperfect breath-hold reproducibility or residual motion of the GTV during treatment. By our estimated dose recalculation, the GTV was consistently covered by the prescription dose (PD), that is, V100% above 0.97 for all patients, and minimum dose to GTV >100% PD for 18 patients and >95% PD for all patients.

Reprint requests to: Billy W. Loo, Jr, MD, PhD, Department of Radiation Oncology and Stanford Cancer Institute, Stanford University School of Medicine, 875 Blake Wilbur Dr, Stanford, CA 94305. Tel: (650) 736-7143; BWLoo@Stanford.edu or Maximilian Diehn, MD, PhD. Tel: (650) 721-1550; Diehn@Stanford.edu.

Conflict of interest: BWL, MD, LX, PGM, and AK receive research support from Varian Medical Systems. BWL and PGM receive research support from RaySearch Laboratories. BWL and PGM have received speaking honoraria from Varian Medical Systems. The authors report other conflicts of interest.

Conclusions—Intrafraction CBCT during VMAT can provide geometric and dosimetric verification of SABR valuable for quality assurance and potentially for treatment adaptation.

Introduction

One of the major challenges in radiation therapy is respiratory tumor motion, primarily in the thorax and abdomen. Respiratory gating is a popular technique to manage tumor motion that limits the radiation to certain parts of the breathing cycle, thereby reducing dose to critical organs (1, 2). The problem with the current standard clinical practice is that the therapeutic beam on/off is controlled solely by some external surrogate (eg, skin surface). This is error-prone because the relationship between the internal target motion and external surrogate can change over time on an inter- and intrafractional basis (3, 4). It is of utmost importance to ensure, by direct measurement if possible, that the moving tumor stays inside the planning target volume (PTV) during the entire delivery process. This is particularly important for stereotactic ablative radiation therapy (SABR), which is characterized by steep dose gradients and large fractional dose (5, 6).

The advent of on-board imaging has provided an enabling tool for treatment verification. Conventionally, this has been predominantly used for pretreatment patient setup purposes (7–10) and occasionally for mid- or post-treatment verification purposes (11–14). Several studies have been performed to investigate its use for intrafraction verification during treatment delivery, relying on fiducial markers for position verification (15–18). Owing to the invasiveness of marker implantation, its indirect nature, and limited information, a safe procedure that directly provides volumetric information about the tumor target is highly desirable. Recently, a few studies have shown the feasibility of acquiring kilovolt cone-beam computed tomography (CBCT) concurrent with megavolt irradiation during volumetric modulated arc therapy (VMAT) (19–21) or by using intermittently triggered kilovolt projections during respiratory-gated VMAT (22). These single-patient studies (phantom study in the case of Ling et al) (20) provide an effective means of verifying tumor positions directly based on soft tissue target, during dose delivery.

In this work, we present our clinical implementation and evaluation of intrafraction CBCT imaging for position and dosimetric verification during VMAT SABR. The key difference from previous studies (11–14) is that the imaging and dose delivery occur at the same time in our study; thus, what is imaged is what is actually being treated. In contrast, all previous studies acquired CBCT either during a pause in delivery or post-treatment rather than while the treatment beam was on, which because of intrafractional motion could result in a discrepancy between the imaged target position and that during actual delivery. In practice, we used the beam-level imaging capability afforded by the Varian TrueBeam linear accelerator (Varian Medical Systems, Palo Alto, CA). The intrafraction CBCT image is used for assessing the geometric accuracy of the SABR treatments directly based on the soft-tissue tumor target. Furthermore, we conduct preliminary dosimetric studies using the geometric information gained from intrafraction volumetric imaging.

Methods and Materials

Patient characteristics

Twenty patients with lung tumors treated with the VMAT technique were identified for inclusion in an institutional review board–approved retrospective study. All patients received SABR treatments in 1, 3, or 4 fractions. Among the 20 patients, 1 patient (patient 18) was treated without gating under free breathing, 4 patients (patients 9, 10, 11, 14) were treated with respiratory gating under free breathing, and the remaining 15 patients were treated under a voluntary biofeedback guided breath-hold protocol. The breath-hold

biofeedback technique was developed by modifying a custom system originally developed for biofeedback guided breathing regularization for improved 4-dimensional (4-D) CT acquisition (23). The mean (±SD) age of all patients was 66 ± 14 years (range: 36–91 years). The size of the gross target volume (GTV) ranges from an equivalent sphere diameter of 0.5 to 4.2 cm. The patient and treatment characteristics are summarized in Table 1.

Patient simulation, treatment planning, setup, and delivery

For patient simulation, either a breath-hold CT scan or 4D CT with 10 respiratory phases was acquired with an 8-slice GE LightSpeed CT scanner (GE Medical Systems, Milwaukee, WI), with an axial slice thickness of 1.25 mm. For patients treated with the breath-hold protocol, the GTV was contoured corresponding to the exhale or inhale phase at breath hold. Consistent with the convention used in Radiation Therapy Oncology Group trials of SABR for lung cancer, the clinical target volume (CTV) was the same as the GTV with no explicit definition of an additional lower dose CTV for microscopic tumor extension; for simplicity, we use GTV in place of CTV hereafter. For patients treated with respiratory gating or motion-inclusive treatment, the ITV was contoured in the maximum intensity projection of the 4-D CT phases within the gating window or the entire respiratory cycle, respectively. For patients treated under breath hold, a margin of 2 mm was added to the GTV to form the ITV (accounting for breath hold variability). In all cases, a margin of 5 mm was added to the ITV to form the PTV. The GTV to PTV expansion was thus ≥7 mm for all patients. A single full- or partial-arc VMAT plan was then optimized using 6 or 10 MV photons without flattening filter, depending on the patient and target geometry. The treatment plan was normalized such that 95% of the PTV receives 100% of the prescription dose. For patient setup, orthogonal kilovolt projections were taken to first align patient anatomy according to bony structures. Volumetric CBCT was then taken during breath hold (in the case of breath-hold treatment) or free breathing, with which the patient was aligned according to the soft tissue tumor target. The appropriate gating window was also determined at this stage to ensure that the tumor target was within the PTV. Finally, the VMAT treatment was delivered using a Varian TrueBeamTM STx Linac, gated by the RPM system. The total number of megaunits varied from 2400 to 6000 MU for all patients. The maximum dose rate was either 1400 MU/min (for 6 MV) or 2400 MU/min (for 10 MV), and the actual dose rate varied from time to time during delivery. The actual delivery time for all patients varied from ~1 to ~4 min.

Image acquisition and CBCT reconstruction

We acquired kilovolt fluoroscopic radiograph projections during the VMAT treatment using the Varian OBI system and iTools software. In clinical mode, the during-treatment kilovolt fluoroscopy acquisition was enabled by scheduling a “during treatment kilovolt” imaging session at the beginning of each fraction. The kilovolt image acquisition protocol was 80 kVp, 44 or 31 mA, and 15 milliseconds. The projections acquired during megavolt beam-on were automatically extracted for image reconstruction and further analysis. Those corresponding to megavolt beam-off were discarded. The angular range of the available cone-beam projections depends on the particular VMAT plan for each patient, and varies between 191° and 359°. We preprocessed the raw projections so that a projection set with a uniform sampling angle was used for image reconstruction. This was done by averaging all projections within every 0.6° of gantry rotation. This sampling is similar to conventional CBCT acquisition. After the treatment was finished, we retrospectively reconstructed volumetric CBCT images using in-house developed software based on the standard filtered backprojection method (24, 25).

Geometric and dosimetric verification of target coverage

To evaluate the target coverage during the VMAT treatment, we calculated the mean target shift in during-treatment CBCT relative to planning CT as well as pretreatment CBCT. This was done by calculating the center of mass of the tumor target in the superior-inferior (SI), left-right (LR), anterior-posterior (AP) directions for each of the 3 image sets. To further assess the dosimetric impact of the target shift during treatment, we estimated the delivered target dose by shifting the entire patient anatomy according to the mean target shift determined earlier. For fractionated treatments, the delivered dose was summed from all fractions with intrafraction image acquisition and then scaled up to the prescription dose. We then calculated the target coverage for GTV (V100%) and the minimum dose to GTV (dose to 0.03 cc) using the estimated delivered dose distribution.

Results

Figure 1 shows the axial, coronal, and sagittal views of the reconstructed CBCT image acquired during dose delivery for patient 1. Both GTV and PTV contours are superimposed on the image. It is clear that the tumor target lies within the PTV during the treatment. However, we observe some degree of tumor blurring in CBCT images (on the order of 2–3 mm upon visual inspection), especially in the axial and sagittal views, indicating imperfect breath-hold reproducibility or residual motion of the target during treatment. Figure 2 shows the coronal and sagittal views of the reconstructed CBCT image for 3 treatment fractions for patient 8. There is some degree of interfraction target shift, which appears to be random.

Figure 3 shows the geometric target shift during treatment from planning CT for all patients. The mean (±SD) absolute target shift from during-treatment CBCT to planning CT was 1.6 ± 1.6, 1.0 ± 0.9, and 1.5 ± 1.4 mm, and the 95th percentile shift was 5.2, 3.1, 3.6 mm along the AP, LR, and SI directions. Of all 20 patients, the maximum target shift was 5.7, 3.6, and 4.9 mm along the AP, LR, and SI directions. Of note, the recorded shift for each fraction represents the average shift of the center of mass of the GTV during that fraction because the CBCT image acquisition time spans the megavolt beam-on time. This indicates that the tumor target was located inside the PTV during the VMAT treatment for this cohort of patients. The target shift between on-treatment and pretreatment CBCT is similar (<1 mm) for all patients, indicating that the target setup based on pretreatment CBCT is accurate. The difference in target shift between different patients was relatively large: for a majority of patients (14 of 20), the target shift was within 2 mm in all 3 directions; in 4 patients the shift, was larger than 4 mm in ≥1 of the directions.

Figure 4 shows the target coverage for GTV and minimum dose to GTV calculated using the estimated delivered dose distributions for all 20 patients. There is essentially no degradation of the V100% for GTV (proportion of GTV covered by the prescription dose) from the planned dose, which is all >0.97. The minimum dose to GTV was >95% of the prescription dose for all patients and >100% for 90% of patients.

Discussion

In this article, we have conducted a clinical study evaluating the geometric and dosimetric accuracies of lung SABR treatments. This is achieved by acquiring CBCT concurrent with dose delivery and reconstructing volumetric patient anatomy during VMAT treatments. A group of 20 patients with lung tumors receiving SABR with a range of motion management techniques (including free breathing, respiratory gating, and breath hold) were analyzed. The GTV was sufficiently covered by the prescription dose for this cohort of patients. Although not assessed in our study, the same methods could be used in future analyses to estimate the delivered coverage to the zone of potential microscopic tumor extension beyond the GTV

and understand what dose is required to sterilize microscopic disease. In this retrospective study, a post-treatment CBCT scan was generally not acquired. In future studies, it would be interesting to compare the post-treatment verification and on-treatment verification.

The large differences in target shift between patients call for individualized margins for SABR. One way to realize this for patients treated with the breath-hold technique could be to acquire repeat breath-hold CT at simulation to determine breath-hold reproducibility, so that a breath-hold ITV can be measured on an individual basis. For patients treated in free breathing or with respiratory gating, this information is partially available in the 4-D CT and could potentially be augmented by repeat 4-D CT at simulation. This potentially could lead to margin reduction for most patients.

The tools developed in this study can be used for retrospective verification or quality assurance purposes in single-fraction SABR treatments. For fractionated treatments, they may be used for adapting treatment plans based on target positioning during treatment and recalculated and accumulated dose. To be useful for treatment intervention or guidance, volumetric images need to be reconstructed on the fly or in real time during treatment. Preliminary studies have shown the feasibility of this approach using on-board imaging device (26, 27). However, comprehensive validations have to be performed before its clinical application.

One caveat of acquiring CBCT during radiation dose delivery is that the projections are contaminated with scatter from the megavolt beam. This may negatively affect the quality of the final reconstructed image. For high-contrast anatomy such as lung, we do not expect the megavolt scatter to be a major issue for geometric and dosimetric evaluations as performed in this study. Methods to deal effectively with the megavolt scatter have been proposed (20, 21), although they more or less require some modification of the existing system hardware and software.

In estimating the delivered dose, we have used the original planning CT and applied an appropriate shift to the entire patient anatomy. Although it is possible to directly use the reconstructed image (provided that it has a sufficient field of view to cover the entire anatomy), CBCT artifacts, noise, and scatter due to both kilovolt and megavolt beams, represent challenging issues for accurate dose calculations. Another confounding factor is residual target motion (see Fig. 1), even when a breath-hold protocol is used. The extent to which this affects the accuracy of subsequent dose calculation should be investigated. Admittedly, the accuracy of the delivered dose in the patient ultimately depends on all factors involved in the radiation therapy process, such as imaging acquisition, target delineation, treatment planning (including dose calculation), treatment delivery, as well as the on-board imaging system. This study aims to address one of the largest uncertainties in lung tumor SABR, intrafractional target motion.

Regarding the imaging dose during VMAT, data from the report of AAPM Task Group 75 (28) suggest that the kilovolt fluoroscopy imaging dose is about 3.5 cGy/min under imaging protocols similar to ours. Because the kilovolt fluoroscopy is continuously on during the entire treatment, the imaging dose is proportional to the actual delivery time (from the moment megavolt is turned on to the end of dose delivery). This translates to a dose of about 0.1 Gy for a 3-min SABR treatment. This number is small compared with the prescription dose, which is typically 10 to 25 Gy per fraction. In addition, using lower mAs and/or lower pulse rate or gating in kilovolt fluoroscopy will further reduce the imaging dose.

Conclusions

We have conducted a clinical study of acquiring CBCT concurrent with VMAT dose delivery and reconstructing volumetric patient anatomy during lung SABR treatments. The on-treatment patient anatomic information gained from beam-level imaging can provide geometric and dosimetric verification of SABR valuable for quality assurance, and potentially treatment adaptation in the future.

Acknowledgments

This project was supported in part by the National Institutes of Health (grant 1K99 166186), Varian Medical Systems, and Li Ka Shing Foundation.

References

1. Shirato H, Shimizu S, Kunieda T, et al. Physical aspects of a real-time tumor-tracking system for gated radiotherapy. Int J Radiat Oncol Biol Phys. 2000; 48:1187–1195. [PubMed: 11072178]
2. Xing L, Thorndyke B, Schreibmann E, et al. Overview of image-guided radiation therapy. Med Dosim. 2006; 31:91–112. [PubMed: 16690451]
3. Ozhasoglu C, Murphy MJ. Issues in respiratory motion compensation during external-beam radiotherapy. Int J Radiat Oncol Biol Phys. 2002; 52:1389–1399. [PubMed: 11955754]
4. Seppenwoolde Y, Shirato H, Kitamura K, et al. Precise and real-time measurement of 3D tumor motion in lung due to breathing and heartbeat, measured during radiotherapy. Int J Radiat Oncol Biol Phys. 2002; 53:822–834. [PubMed: 12095547]
5. Timmerman RD, Kavanagh BD, Cho LC, et al. Stereotactic body radiation therapy in multiple organ sites. J Clin Oncol. 2007; 25:947–952. [PubMed: 17350943]
6. Dawson LA, Eccles C, Bissonnette JP, et al. Accuracy of daily image guidance for hypofractionated liver radiotherapy with active breathing control. Int J Radiat Oncol Biol Phys. 2005; 62:1247–1252. [PubMed: 15990028]
7. Wang Z, Nelson JW, Yoo S, et al. Refinement of treatment setup and target localization accuracy using three-dimensional cone-beam computed tomography for stereotactic body radiotherapy. Int J Radiat Oncol Biol Phys. 2009; 73:571–577. [PubMed: 19147021]
8. Pouliot J, Bani-Hashemi A, Chen J, et al. Low-dose megavoltage cone-beam CT for radiation therapy. Int J Radiat Oncol Biol Phys. 2005; 61:552–560. [PubMed: 15736320]
9. Sonke JJ, Zijp L, Remeijer P, et al. Respiratory correlated cone beam CT. Med Phys. 2005; 32:1176–1186. [PubMed: 15895601]
10. Li T, Xing L, Munro P, et al. Four-dimensional cone-beam computed tomography using an on-board imager. Med Phys. 2006; 33:3825–3833. [PubMed: 17089847]
11. Bissonnette JP, Franks KN, Purdie TG, et al. Quantifying interfraction and intrafraction tumor motion in lung stereotactic body radiotherapy using respiration-correlated cone beam computed tomography. Int J Radiat Oncol Biol Phys. 2009; 75:688–695. [PubMed: 19395200]
12. Shah C, Grills IS, Kestin LL, et al. Intrafraction variation of mean tumor position during image-guided hypofractionated stereotactic body radiotherapy for lung cancer. Int J Radiat Oncol Biol Phys. 2012; 82:1636–1641. [PubMed: 21489715]
13. Sonke JJ, Rossi M, Wolthaus J, et al. Frameless stereotactic body radiotherapy for lung cancer using four-dimensional cone beam CT guidance. Int J Radiat Oncol Biol Phys. 2009; 74:567–574. [PubMed: 19046825]
14. Li W, Purdie TG, Taremi M, et al. Effect of immobilization and performance status on intrafraction motion for stereotactic lung radiotherapy: Analysis of 133 patients. Int J Radiat Oncol Biol Phys. 2011; 81:1568–1575. [PubMed: 21075559]
15. Adamson J, Wu Q. Prostate intrafraction motion assessed by simultaneous kilovoltage fluoroscopy at megavoltage delivery I: Clinical observations and pattern analysis. Int J Radiat Oncol Biol Phys. 2010; 78:1563–1570. [PubMed: 20579817]

16. Berbeco RI, Hacker F, Ionascu D, et al. Clinical feasibility of using an EPID in CINE mode for image-guided verification of stereotactic body radiotherapy. Int J Radiat Oncol Biol Phys. 2007; 69:258–266. [PubMed: 17707280]
17. Tai A, Christensen JD, Gore E, et al. Gated treatment delivery verification with on-line megavoltage fluoroscopy. Int J Radiat Oncol Biol Phys. 2010; 76:1592–1598. [PubMed: 20133069]
18. Li R, Mok E, Chang DT, et al. Intrafraction verification of gated RapidArc by using beam-level kilovoltage X-ray images. Int J Radiat Oncol Biol Phys. 2012; 83:e709–e715. [PubMed: 22554582]
19. Nakagawa K, Haga A, Shiraishi K, et al. First clinical cone-beam CT imaging during volumetric modulated arc therapy. Radiother Oncol. 2009; 90:422–423. [PubMed: 19062117]
20. Ling C, Zhang P, Etmektzoglou T, et al. Acquisition of MV-scatter-free kilovoltage CBCT images during RapidArc or VMAT. Radiother Oncol. 2011; 100:145–149. [PubMed: 21821301]
21. van Herk M, Ploeger L, Sonke JJ. A novel method for megavoltage scatter correction in cone-beam CT acquired concurrent with rotational irradiation. Radiother Oncol. 2011; 100:365–369. [PubMed: 21924785]
22. Choi K, Koong A, Xing L, et al. First study of on-treatment volumetric imaging during respiratory gated VMAT. Med Phys. 2013; 40:040701. [PubMed: 23556870]
23. Venkat RB, Sawant A, Suh Y, et al. Development and preliminary evaluation of a prototype audiovisual biofeedback device incorporating a patient-specific guiding waveform. Phys Med Biol. 2008; 53:N197–N208. [PubMed: 18475007]
24. Feldkamp LA, Davis LC, Kress JW. Practical cone-beam algorithm. J Opt Soc Am. 1984; 1:612–619.
25. Kak, A.; Slaney, M. Principles of Computerized Tomographic Imaging. Philadelphia: Society for Industrial and Applied Mathematics; 2001.
26. Li R, Jia X, Lewis JH, et al. Real-time volumetric image reconstruction and 3D tumor localization based on a single x-ray projection image for lung cancer radiotherapy. Med Phys. 2010; 37:2822–2826. [PubMed: 20632593]
27. Li R, Lewis JH, Jia X, et al. 3D tumor localization through real-time volumetric x-ray imaging for lung cancer radiotherapy. Med Phys. 2011; 38:2783–2794. [PubMed: 21776815]
28. Murphy MJ, Balter J, Balter S, et al. The management of imaging dose during image-guided radiotherapy: Report of the AAPM Task Group 75. Med Phys. 2007; 34:4041–4063. [PubMed: 17985650]

Summary

We developed and clinically evaluated an intrafraction cone beam computed tomography technique for geometric and dosimetric verification of lung tumor stereotactic ablative radiation therapy. In 20 patients treated with a range of motion management techniques, the gross tumor volume was found to be within the planning target volume and well covered by the prescription dose in all cases. Intrafraction cone beam computed tomography should be valuable for individual patient quality assurance and potentially for treatment adaptation.

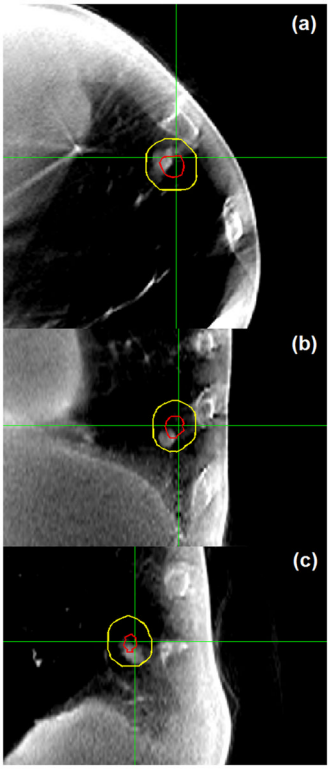

Fig. 1.
Axial, coronal, and sagittal views of the reconstructed cone beam computed tomography image (zoomed in on the gross tumor volume with a diameter of ~6 mm) for patient 1. Both gross tumor volume and planning target volume contours are superimposed on the image. Target smearing is visible in axial and sagittal views. This verifies that the intrafraction tumor position is within the planning target volume.

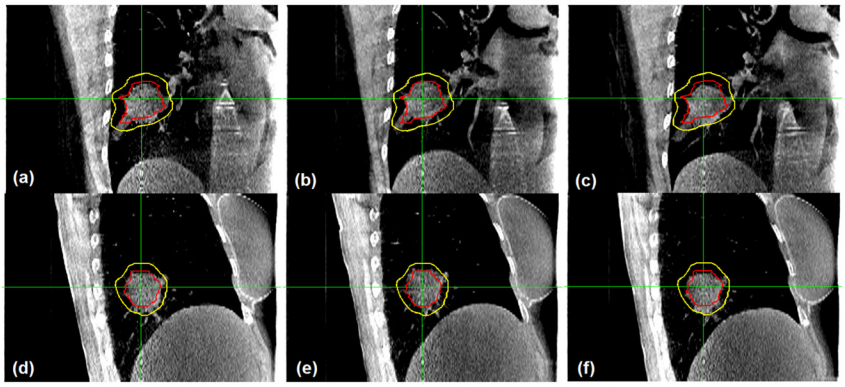

Fig. 2.

Coronal (a–c) and sagittal (d–f) views of the reconstructed cone beam computed tomography image for 3 treatment fractions for patient 8. Both gross tumor volume and planning target volume contours are superimposed on the image. This verifies that the intrafraction tumor position is within the planning target volume during each fraction.

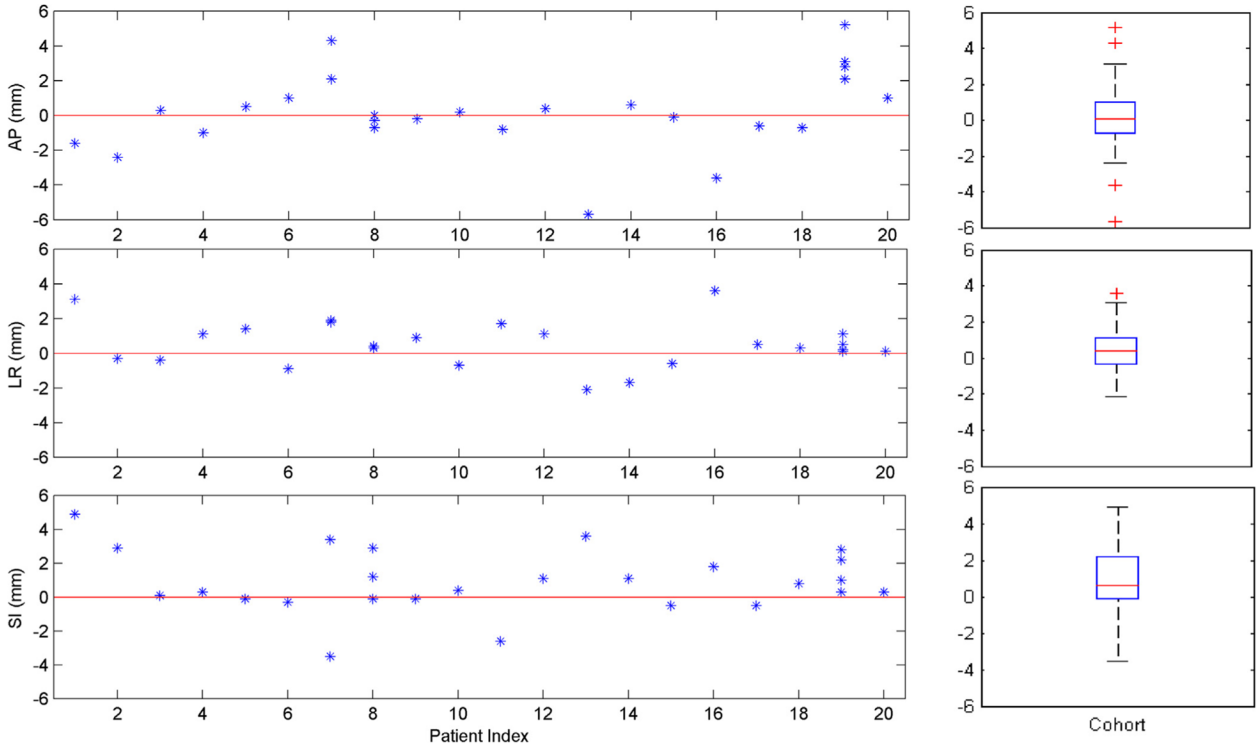

Fig. 3.

Geometric mean target shift during treatment relative to planning computed tomography for all patients (left panel), as well as the boxplot for the patient cohort (right panel). On each box, the central mark is the median, the edges of the box are the 25th and 75th percentiles, the whiskers extend to the most extreme data points not considered outliers (~2.7 SD or 99.3% coverage for normally distributed data), and outliers are plotted individually.

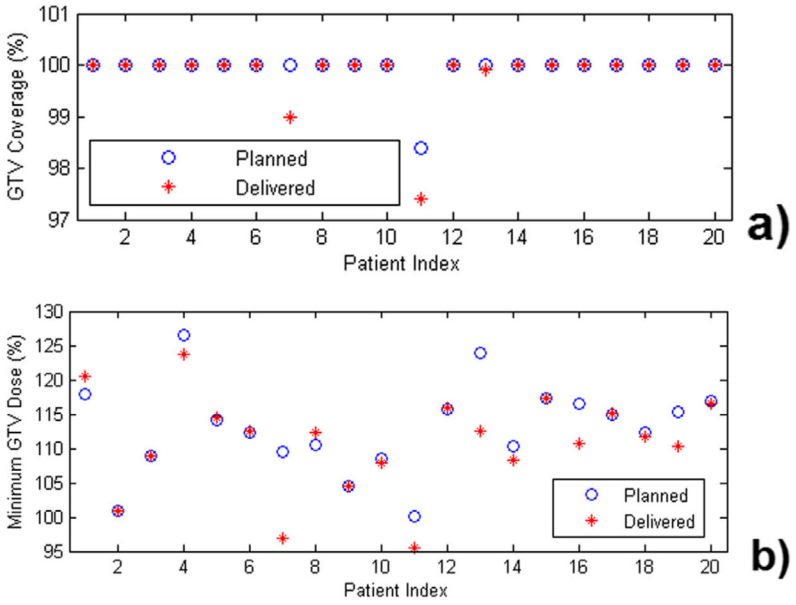

Fig. 4.

Gross tumor volume coverage (GTV) (a) and minimum dose to GTV (b), calculated from the estimated delivered dose distributions for all patients. The minimum dose is dose to 0.03 cm^3 rather than to a single voxel. The delivered dose distribution is estimated by applying the mean target shift during treatment to the entire patient anatomy in planning computed tomography. In all cases, the GTV is well covered by the prescription dose. AP = anterior-posterior; LR = left-right; SI = superior-inferior.

Table 1

Patient and treatment characteristics

Patient index	Age (y)	Gender	Tumor site	Motion management	Prescription (Gy)	No. of fractions acquired	No. of breaths per fraction	Average beam on time per breath (s)
1	36	M	LLL	BH	25 × 1	1	3	33
2	72	F	LLL	BH	25 × 1	1	8	14
3	63	F	RUL	BH	10 × 4	1	3	34
4	47	M	LLL	BH	25 × 1	1	9	22
5	65	M	LLL	BH	10 × 4	1	2	26
6	60	F	LLL	BH	25 × 1	1	6	23
7	40	F	RLL	BH	18 × 3	2	2	50
8	56	F	RLL	BH	12.5 × 4	3	2	38
9	91	F	LUL	G	12.5 × 4	1	42	2.1
10	71	F	RUL	G	25 × 1	1	33	5.4
11	63	F	LLL	G	10 × 4	1	15	4.2
12	79	M	RLL	BH	25 × 1	1	6	21
13	75	M	RLL	BH	25 × 1	1	7	14
14	85	F	LLL	G	25 × 1	1	61	2.5
15	69	F	RML	BH	25 × 1	1	1	84
16	73	F	LLL	BH	25 × 1	1	10	9.4
17	73	M	RLL	BH	25 × 1	1	7	24
18	62	M	RUL	FB	25 × 1	1	-	-
19	85	M	RLL	BH	12.5 × 4	4	8	11
20	62	M	LLL	BH	12.5 × 4	1	1	65

Abbreviations: BH = breath hold; FB = free breathing; G = gating; LLL = left lower lobe; RLL = right lower lobe; RML = right middle lobe; RUL = right upper lobe.